Local Probe and Conduction Distribution of Proton Exchange Membranes

ARTICLE *in* THE JOURNAL OF PHYSICAL CHEMISTRY B · JULY 2007

Impact Factor: 3.3 · DOI: 10.1021/jp0706230 · Source: PubMed

Local Probe and Conduction Distribution of Proton Exchange Membranes

Xin Xie, Osung Kwon, and Da-Ming Zhu*

Department of Physics, University of Missouri - Kansas City, Kansas City, Missouri 64110

Trung Van Nguyen and Guangyu Lin

Department of Chemical and Petroleum Engineering, University of Kansas, Lawrence, Kansas 66045

Received: January 24, 2007; In Final Form: March 23, 2007

Proton exchange membranes (Nafion) have been studied using current sensing atomic force microscopy to examine the correlation between the surface morphology and the ionic domains, and to probe the local ionic conduction distribution in the membranes. It is found that the local ionic conduction generated from the current sensing images follows a Gaussian-like distribution, with the peak value and the width of the distribution increasing with the relative humidity in the sample chamber and, thus, the water content in the membranes. Two types of Nafion membranes, Nafion 112 and Nafion 117, were studied using the method. The implications of the distribution in relation to the ionic conducting channels in the membranes are discussed.

1. Introduction

Proton exchange membranes (PEM) play an essential role in many areas of technology, including batteries, fuel cells, electrochemical devices, and sensors.[1−7] Currently, the most widely used proton exchange membrane is Nafion, a commercially available perfluorosulphonate cation exchange membrane, manufactured by DuPont and Co., which displays good performance in electrochemical devices and fuel cell applications.[8] The properties of Nafion have been studied in recent years using various techniques such as X-ray and neutron scattering,[8−12] electron microscopy, and positron annihilation spectroscopy.[13,14] Its structure is found to be inhomogeneous, consisting of hydrophobic fluorinated polymer Teflon backbones, attached pendant side chains, and sulfonic acidic groups ($-SO_3H$) at the side chains terminals. The structure changes quite drastically with the membrane's hydration states and/or the external variables.[19−27] A number of studies have been performed to devise sophisticated models linking macroscopic transport properties to the molecular level structures of the membranes.[19−21,29] These models describe Nafion more or less as a solid matrix constituting of polymer backbones interspersed with randomly distributed self-assembled clusters made of flexible side chains terminated with sulfonate head groups. With the water uptake, the head groups on the side chains enclose the water particles, forming inverted micelles. The size of the micelles increases with the amount of water adsorbed, and they gradually become connected by narrow channels. At a certain humidity level, the percolation network is established and the proton conductivity starts to grow with the water content. Several other types of perfluorosulphonate cation membranes that have been developed in recent years were found to have structures and properties similar to that of Nafion membranes.[30]

Although these theoretical models appear to be capable of describing most of the experimentally observed properties of PEMs, many details of these properties remain in debate.[30] In particular, while it is known that Nafion and most other PEMs are intrinsically heterogeneous, the properties of these PEMs were studied in such ways that only the averaged performance could be extracted. Many predictions of the models remain speculative, such as the suggestion that the ionic conductance of a PEM is controlled by the necks between hydrophilic clusters.[29] In order to obtain a strategy for synthesizing new PEMs having significantly improved properties and performance, a fundamental understanding of the transport mechanisms and their relationship with the microscopic structures of the membranes is apparently required.[2,30] From an experimental point of view, in order to improve the understanding of the ion transport properties, new approaches are needed that can provide quantitative measurements, at microscopic or mesoscopic levels, of ionic transport in the conducting networks of a PEM.[2]

Among various experimental techniques, local probes, such as atomic force microscopy (AFM) and its alternative versions, have proven to be powerful tools for investigating materials with inhomogeneous properties.[27,28] AFM advances have enabled the technology to be used to map electrical, mechanical, magnetic, chemical, and, to some extent, biological properties with nanometer-scale resolution. Indeed, AFM has been employed in the studies of Nafion membranes, with the goal of resolving the cluster structures and determining the cluster distributions in the membranes.[8−12,28] The results from the studies that employ both AFM and transmission electron microscopy (TEM) have established the presence of ionic clustering of size in the range of 3−10 nm and with approximately spherical shapes in Nafion membranes.[11,12,27] However, it is difficult by using AFM alone to determine whether the ionic clusters on the membrane surface resolved in AFM images are active or not. Only ionic clusters that are connected to the ionic network within the membrane allowing proton to transport from one surface of the membrane to the other are considered active, or to have ionic activity, and thereby contribute to the ionic transport in the membranes. The first investigation of the surface ionic activity of Nafion was carried out by Allan Bard's group using electrochemical scanning microscopy (SECM).[31] They found that only localized activity existed on the membrane surface.[31] A more detailed SECM-based analytical method was subsequently employed in char-

* Corresponding author.

10.1021/jp0706230 CCC: $37.00
Published on Web 05/16/2007

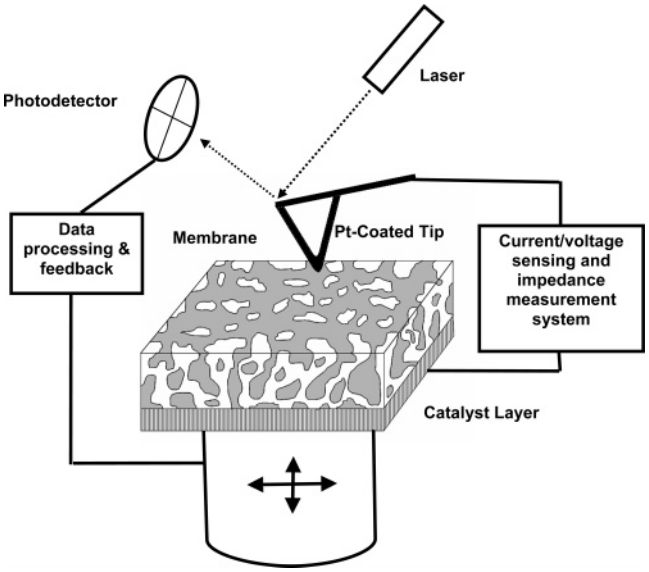

Figure 1. Illustration of the experimental setup of the current sensing atomic force microscopy study of Nafion membranes.

acterizing mica/Nafion membranes for analyzing electro-osmotic and diffusive fluxes of ions in real time.[32] More recently, impedance atomic force microscopy and conductive probe atomic force microscopy, techniques that allow simultaneously imaging surface morphology and local impedance on the surface, was used in a study of Nafion membranes.[28,33] The results unambiguously identify surface ionic active domains on Nafion surfaces.[28,33] In our previously reported work, we have demonstrated that current sensing atomic force microscopy (CSAFM), which is a DC version of the impedance AFM technique, can be used to directly measure the surface ionic activity of proton conducting membranes.[19] The results obtained by us show that the surface ionic activity depends significantly on the relative humidity in the gas phase. At low relative humidity, most of the membrane surface is inactive.[19] At high relative humidity, many regions on the surface become active. However, these regions are still only a fraction of the total surface.[19]

In this paper we will present more complete and detailed results of the study of Nafion membranes using CSAFM. In our study, the surface morphology and the current sensing images on the same area of a Nafion membrane were acquired simultaneously. The results show that while the surface morphology varies significantly from area to area depending on the local surface roughness and the crumple of the membrane, the conduction distributions generated from the ionic current image display a robust Gaussian-like behavior, with the peak value and the peak width increasing with relative humidity. The implications of the conduction distribution will be analyzed and discussed in the following sections.

2. Experimental Methods

Figure 1 illustrates the experimental CSAFM setup for the study of Nafion membranes. The essential component in a CSAFM is a sensitive electric current measuring loop added to the conventional AFM. The current measuring loop connects the conducting AFM tip to a sample, with a 10^{-12} Ampere sensitivity in current measurement. The CSAFM system used in this study was one designed specifically for chemical and biological applications.[34] The unique aspect of the system is an environmental sample chamber that is isolated from the scanner and connected to a gas handling system, allowing imaging under a controlled and variable gas composition. The humidity in the chamber was controlled by adjusting the valves that connect to a water vapor source and a pumping system, and was monitored through a simple humidity meter which is sensitive for measuring relative humidity in a range from 20% to about 90%. The AFM tip used was coated with a layer of platinum which served as a catalyst particle in contact with the membranes.

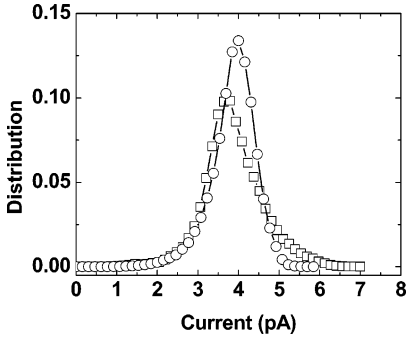

Figure 2. The distributions of ionic conduction on a Nafion 117 membrane derived from two images obtained using two randomly chosen probes and at two different locations. The relative humidity in the sample chamber was 30%.

Nafion membranes received from Dupont were cleaned following a standard procedure. One electrode which is made of platinum powder deposited on a carbon /substrate was hot compressed onto the one side of the Nafion membrane, forming a Carbon/Pt/Nafion anode. The carbon substrate is porous, allowing gases to permeate through. The carbon substrate was then attached to the CSAFM sample stage using conducting carbon glues. The tip/membrane/electrode assembly was immersed in air at a controlled relative humidity level. A bias voltage was applied between the porous electrode on one side of the membrane and the conducting tip. As the tip moved across a membrane surface, the detected current formed a spatially resolved current sensing image, together with the morphology image generated by the contact mode AFM.

During the measurements, a Pt-coated AFM tip was in gentle contact with the bare side of the Nafion membrane, with a minimum force needed (typically in the nanoNewton range). The platinum layer on the AFM tip acts as another electrode (cathode) on the membrane, as shown in Figure 1. The contact area between the tip and the membrane is determined by the radius of the tip, which is about 5 nm, as quoted by the manufacturer.[34] The surrounding open space allows reaction gases accessing the platinum layer between the tip and the membrane. The Tip/Pt/Nafion/Pt/Carbon assembly forms essentially a miniature fuel cell. In principle, as the Pt-coated tip moves across the membrane, the performance of the membrane can be evaluated at a nanometer scale using this instrument.

Since the Nafion membranes used in this study were hot-pressed onto carbon porous substrates, their surface morphology adopted that of the carbon substrates which were porous with pore sizes ranging from a few nanometers to a few micrometers. The contact mode imaging used in this study traces out the surface contour under a constant applied force. Thus, it is not possible to resolve individual ionic clusters from the morphology images in this study. For current sensing images, the resolution is determined by the contact area between the probe tip and the active ionic clusters. Thus, the resolution for current sensing images is expected to be better than that of the morphology images. But the area of the AFM tip apex used in this study is several times larger than the size of ionic clusters, and the water meniscus formed around the probe tip further increases the effective probe size. Thus, it is also difficult to unambiguously

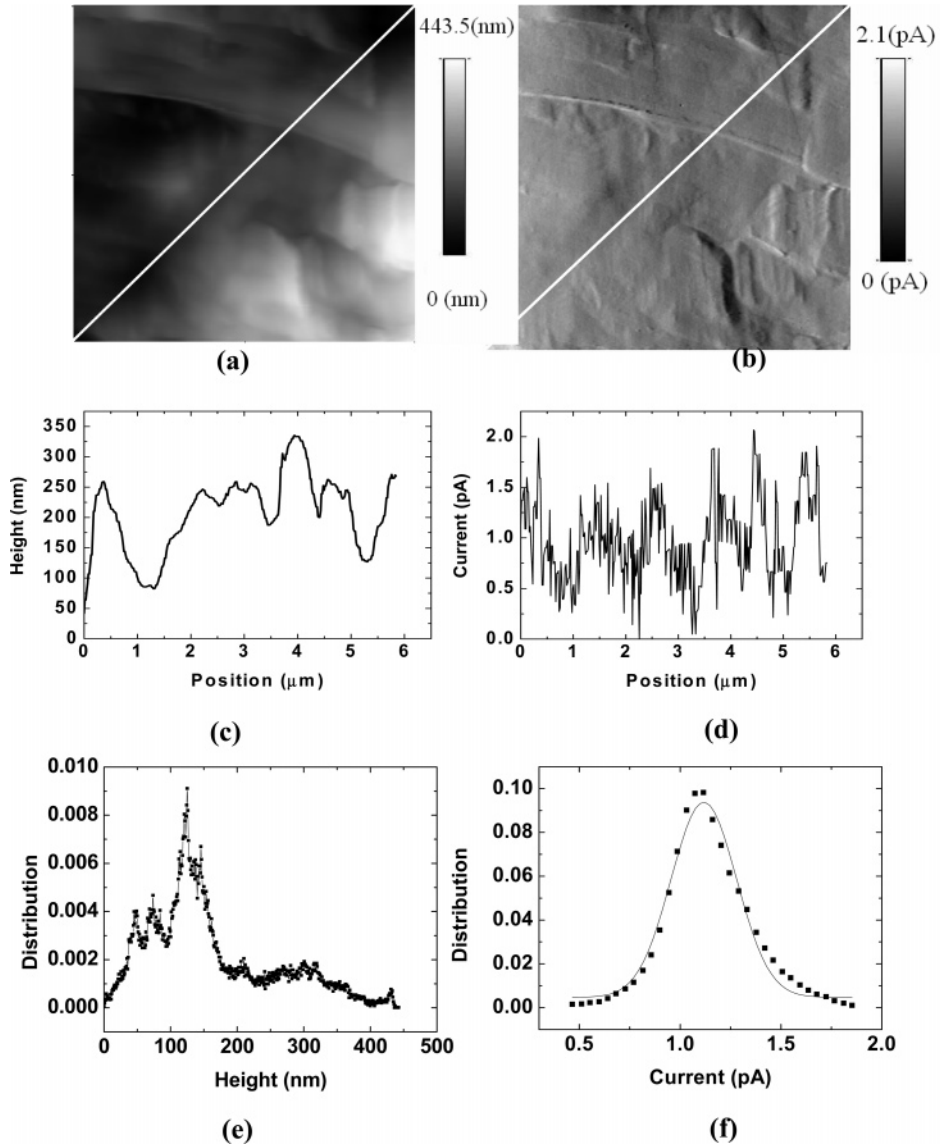

Figure 3. (a) Topographic image of a Nafion 112 membrane at a relative humidity of 30%. (b) Current sensing image of the membrane obtained simultaneously as that in panel a, under a bias voltage of −1.5V. The scan size is 4 μm × 4 μm for both images. (c, d) Profiles along the diagonal lines indicated in panels a and b. (e, f) Surface height and conduction distribution derived from the topographic and current sensing images. The line in the conduction distribution is a Gaussian fit.

resolve individual ionic clusters from the current sensing images using the current experimental setup. However, assuming that the variation of mechanical stiffness on the membrane surface is small, a constant force mode would maintain a constant contact area between the tip and the membrane surface during imaging. Then the current sensing image would reflect the variation of the local ionic activity on the surface and the ionic conductivity across the membrane, because proton conduction occurs once the tip makes contact with an active ionic cluster or domain which is connected with the ionic cluster network across the membrane. In our study, special cares were taken to maintain a constant force applied to the tip during imaging by optimizing the gain parameters of the AFM. Thus, although it is not possible to resolve individual ionic clusters in this study, the conduction distributions generated from current sensing images (simply counting the occurrence of current values across the images) offers a novel approach in statistically analyzing the distribution of the active ionic clusters on a membrane surface and their connection with the random ionic network inside the membrane. We found that the current sensing images obtained using the same fresh tip were reproducible, and the general features shown in the images obtained using different fresh tips under the same condition are similar. Figure 2 shows the conduction distributions generated from two proton conduction images obtained on the same Nafion 117 membrane sample under the same conditions but using two different probe tips. We noticed that as a tip is repeatedly used, sudden deteriorations in the conduction of the membranes were observed. We attribute this as due to the wearing of the Pt film at the end of the probe tip.

3. Results

Figures 3a,b and 4a,b are morphology and current sensing images of the same area of a Nafion 112 membrane obtained under relative humidity of 30% and 80%, respectively. Detailed characteristic features in the surface morphology and current sensing images can be more easily seen from the surface height and current profiles (Figures 3c,d and 4c,d) across the images

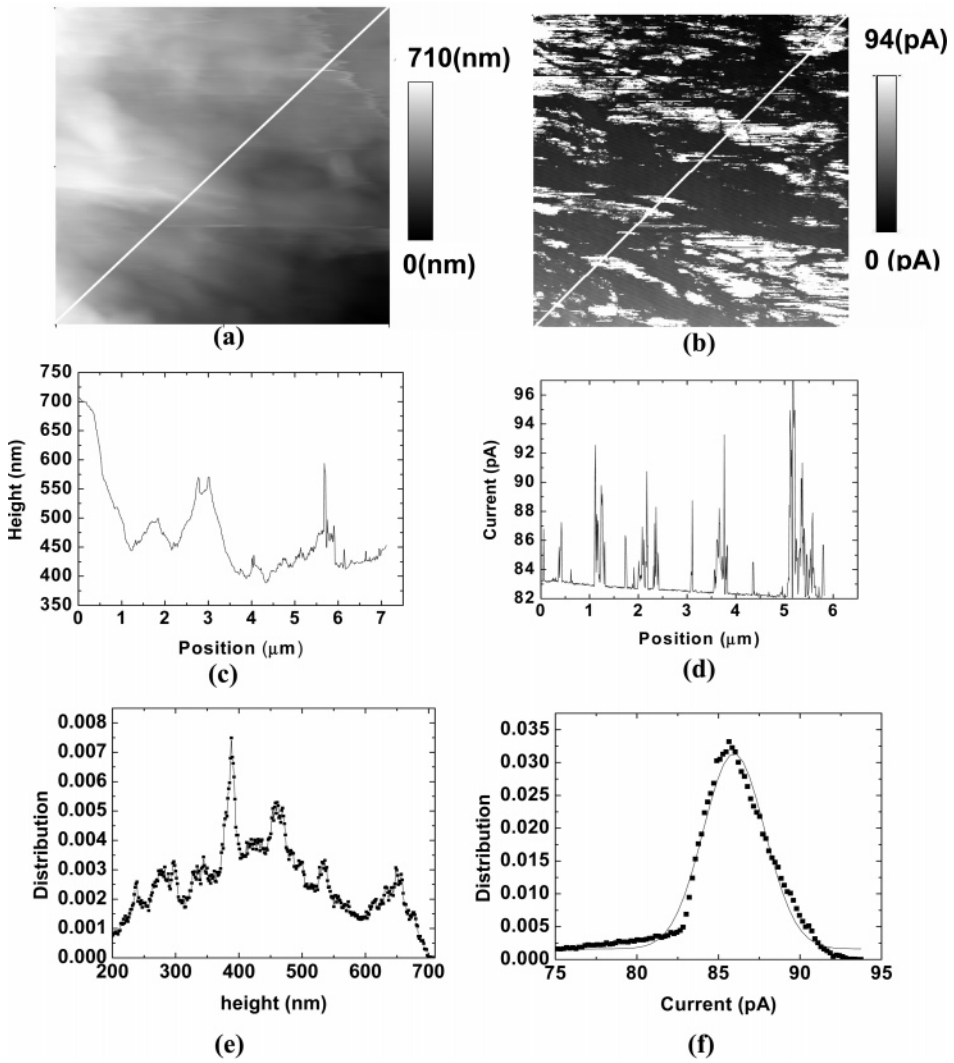

Figure 4. (a) Topographic image of a Nafion 112 membrane at a relative humidity of 80%. (b) Current sensing image of the membrane obtained simultaneously as that in panel a, under a bias voltage of −1.5 V. The scan size is 4 μm × 4 μm for both images. (c, d) Profiles along the diagonal lines indicated in panels a and b. (e, f) Surface height and conduction distribution derived from the topographic and current sensing images. The line in the conduction distribution is a Gaussian fit.

along the indicated lines, and from the surface height and conduction distributions generated from the surface morphology and current sensing images, respectively. Figures 3e,f and 4e,f plot these distributions obtained from the corresponding morphology and current sensing images shown in Figures 3a,b and in 4a,b. It is interesting to note that although the surface height distribution shows, typically, a main broad peak together with many side peaks, and that the overall features of the distribution vary significantly from the scanned area to area, the shape of the conduction distribution is always Gaussian-like. The peak value and the width of the distribution vary within a factor of about two from different scanned areas on the membrane and by using different probe tips. The results obtain on Nafion 117 membranes show similar features. Figure 5 shows a typical surface morphology image (Figure 5a), together with a simultaneously obtained current sensing image (Figure 5b) on a Nafion 117 membrane. To show the characteristic difference between the two types of the images, the height and current sensing profiles along the lines crossing the images are displayed in Figures 5c,d, and the surface height and conduction distributions derived from the images are shown in Figures 5e,f. The conduction profile shows that the variation of the conduction is more rugged than that in the surface height profile and occurs at a length scale much smaller than a micrometer. The results for Nafion 112 and Nafion 117 membranes are very similar at low relative humidity. At higher relative humidity, the averaged ionic conduction in Nafion 112 seems to be lower than that in Nafion 117.

The images obtained in this study reveal that there is little correlation (those reflect the major macroscopic features on the membranes, such as the wrinkles displayed in Figures 3a,b) between the surface morphology and the ionic activity or conductivity of a Nafion membrane. This result and the current−voltage curves (not reported here) are in agreement with the results that were reported in a recent work using a similar approach.[28]

4. Discussion

a. Possible Origin of the Observed Conduction Gaussian Distribution. It is interesting to note that although the surface height distribution in an image of the Nafion membrane can vary significantly from sample to sample, the conduction distribution generated from the current sensing image appear to follow approximately a Gaussian distribution. The measured conduction distribution is related to the distribution of active ionic clusters on the surface and the percolated ionic network in the membrane. It is generally believed that the ionic channels

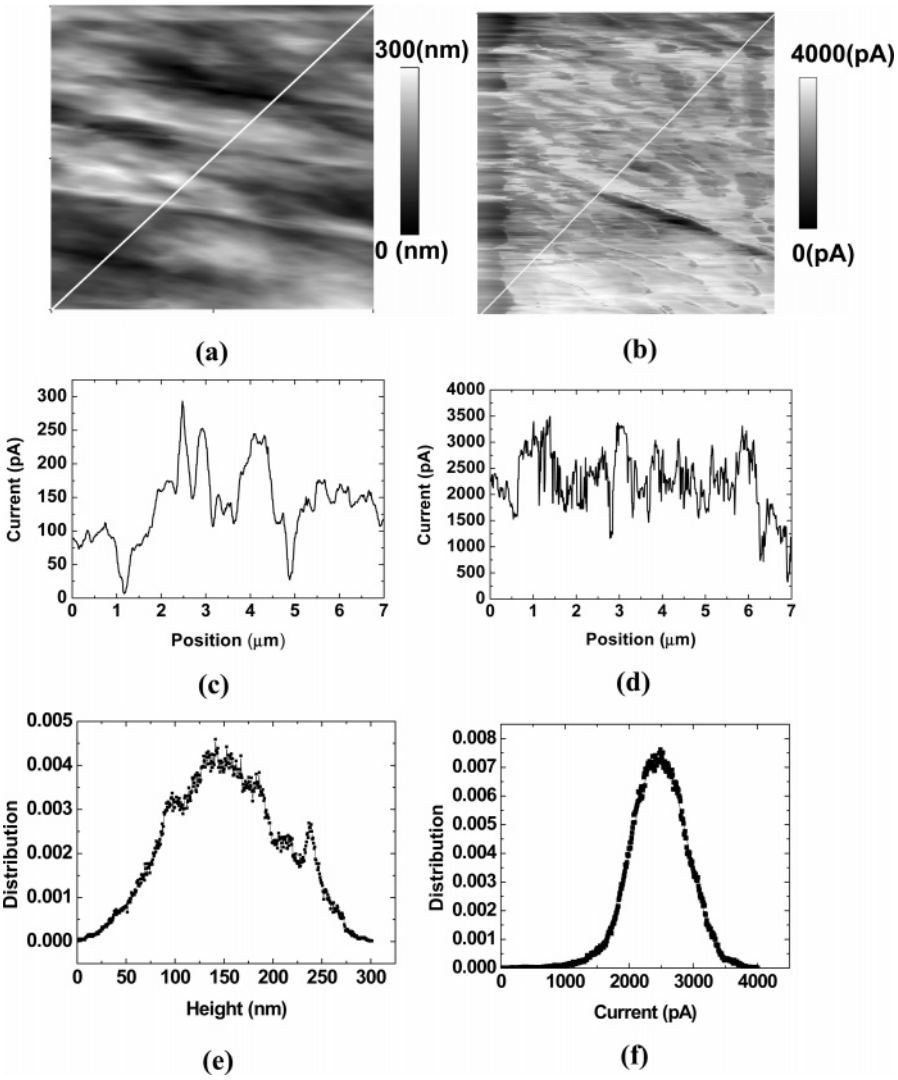

Figure 5. (a, b) Topographic and current sensing images of a Nafion 117 membrane at a relative humidity of 80%. The scan size is 5 μm × 5 μm. (c, d) Profiles along the diagonal lines indicated in panels a and b. (e, f) Surface height and the conduction distributions derived from the images shown in panels a and b. The lines in the conduction distributions are Gaussian fits.

in a Nafion membrane are randomly connected. For membranes of thickness much larger than the characteristic size of a single channel, the ionic pathway from one size of the membrane connected by the probe branch out through a large number of channels as it reach the other side of the membrane which is connected through a planar catalyst layer. Thus, the effect of the random percolation network is the contribution of a constant background as the probe makes a contact with one of the ionic clusters, and the conduction distribution is mainly determined by the distribution of the contact areas between the probe and the clusters. The Gaussian-like distribution obtained in this study reflects the randomness in the contact areas between the probe and the ionic active clusters on the membrane surface. If the size of the active ionic cluster is smaller than the probe size and the cluster density is low or if the probe size is much smaller that of the active clusters, then the probe either makes a contact or miss the clusters, the distribution should be sharp. On the other hand, if the probe size is larger than that of the clusters and the density of the cluster is large so that the probe will always have some contact with some of the active clusters on the surface, then a broad distribution is expected. A quantitative assessment of the cluster distribution in the membrane using the measured conduction distribution requires more complicated analysis and simulations. Our preliminary analysis found that

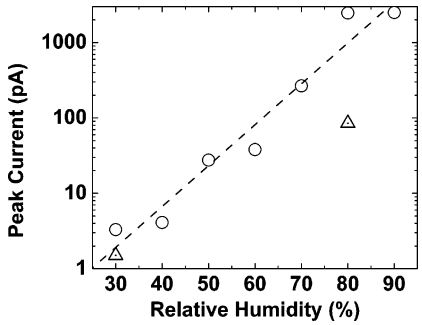

Figure 6. The peak values of the conduction distributions derived from current sensing images of a Nafion 112 (○) and a Nafion 117 (△) membranes measured at different relative humidity in the sample chamber. The dashed line is the guide to the eyes.

the approach of using a local probe to characterize the conduction distribution might also be useful to study the conduction behaviors of random nanotube bundles.[35] The details of the work will be presented elsewhere.[35]

b. Humidity Dependence of the Ionic Conduction Distribution. The conduction distributions obtained from the current sensing images were fitted with Gaussian functions. Figure 6 plots the peak values of the conduction distribution for the Nafion membranes versus the relative humidity in the sample

chamber. The peak value of the conductivity distribution increases with the humidity rapidly. The increase of the peak value of the distribution with the relative humidity is obviously related to the increase of the proton conductance through the ionic network in the membrane as it becomes hydrated. The results from previous studies show that when the membrane is dry, individual clusters have sizes around 3−5 nm, and are weakly connected.[2−6] As the humidity rises, the water content in the membranes increases, the size of ionic cluster appear to rise, the size of the clusters reaches about 30 nm upon hydration and some of the clusters aggregate together.[24] Also, high relative humidity level may allow formation of new active ionic clusters and the nonuniform expansion of the existing active ionic clusters by branching out in directions where chemical environment may favor the formation of one-dimensional ionic channel.[19−27] The increasing of cluster sizes and the formation of the new clusters significantly increases the interconnection between clusters, and thus the conductivity.[5,6] The surface ionic activity on the membrane also plays an important role. These ionic groups are mostly inactive and are not connected with the inner ionic clusters in the membrane when the humidity is low. With increasing humidity, they become increasingly active at higher humidity. Some of the ionic groups are connected to the inner cluster networks and these groups will help the inner cluster networks transport protons, increasing the conductivity significantly.[23−25]

For a Gaussian distribution, the peak value corresponds to the averaged value of the distribution variable. Thus, the peak value shown in Figure 6 should correspond to the averaged conductivity across the membrane. The increase of the peak value of the conduction distribution is consistent with the increase of the specific conductivity of a similar Nafion membrane with relative humidity, measured using a four-probe method.[29,35] If we assume that the ionic transport is mainly carried out by the part of the membrane in between the tip of a diameter of about 10 nm and the opposite electrode, the magnitude of specific conductivity of Nafion membranes derived from the conductance image is comparable to that measured macroscopically.[35] To compare our results with the magnitude of impedance obtained from the recent study using impedance AFM,[33] the resistance derived from the images presented here is roughly 1 order of magnitude larger than the magnitude of the impedance derived from the impedance imaging using AFM on the same type of Nafion membranes. However, the force applied to the membrane from the probe in the impedance AFM work is about 3 orders of magnitude larger than what we used in this study. We imaged the Nafion membranes under different applied forces through the probe tip, and found that the conduction distribution remains to be Gaussian-like while the peak value increases by a factor of about two as the force is increased by an order of a magnitude. Thus, the average specific conductivity of Nafion and its dependence on the relative humidity presented here are consistent with the currently existing results obtained on the membranes.

In Figure 7, we plot the half width at maximum height (HWMH) of the conduction distributions versus the relative humidity in the sample chamber for the two types of Nafion membranes studied. The width of the distribution is relatively narrow at low relative humidity. Similar to the behavior of peak value of the distribution, the width also rises with the relative humidity. As mentioned above, the results from previous studies indicate that as the water content in the membrane is low, the size of the clusters is about a few nanometers, which is smaller than the size of the probe tip used, and as the membranes become hydrated, the clusters become aggregated, and their size increases to about tens of nanometers, which is comparable to the probe size.[19−27] Thus, qualitatively, the rise of the HWMH confirms what we know about the variation of the ionic clusters in response to the water content increase in Nafion membranes. In recent work by James et al., a cluster counting algorithm was used in analyzing the AFM images of Nafion membranes obtained using a tapping mode.[11,12] A tapping mode method generates both topography and phase images; the latter maps the variation of rigidity across a sample surface. The phase distribution of the images, which was attributed to the cluster distribution, was found to sharply peak at low humidity, and broaden as the humidity rises.[11,12] The width of the phase contrast rises by a factor 4 as the humidity increases from 9% to 34%.[11,12] This rate of increase in the width of phase contrast distribution is similar to what we have found in the HWMH of the ionic conduction distribution, as shown in Figure 7.

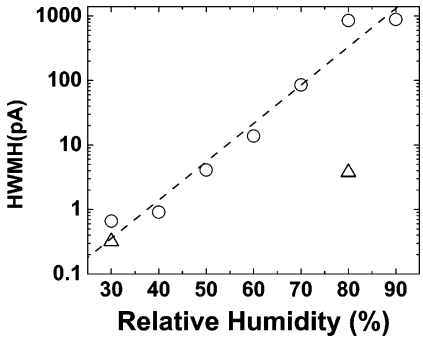

Figure 7. The half width at maximum height (HWMH) of the conduction distributions derived from current sensing images of the same Nafion 112 (○) and Nafion 117 (△) membranes measured at different relative humidity in the sample chamber. The dashed line is to guide the eye.

It should be noted that in the study reported here, the membrane samples were immersed in a controlled humidity environment, and thin water films were expected to exist on the membrane surface.[31,37] Such films should not contribute significantly to the contrast in the current sensing images, because the films are connected around the surface of the membrane which covers many hydrophilic and hydrophobic regions. But the water meniscus around the probe tip would increase the effective contact area between the tip and the membrane (or the effective size of the probe tip), which may contribute significantly to the increase of the peak value and the width of the conduction distribution measured by CSAFM.

Conclusions

We have studied Nafion membranes using current sensing atomic force microscopy (CSAFM). The results obtained show that CSAFM is an effective tool for revealing local conductivity variation and conductivity distribution in the membranes. It is found that the ionic conduction distribution follows approximately a Gaussian function, with the peak and half width of the peak increasing exponentially with relative humidity. The increase of the peak and the width with the relative humidity are consistent with current knowledge on the Nafion membranes. The approach may provide a new way in characterizing and studying ion exchange membranes.

Acknowledgment. This work is supported in part by a grant from Research Corporation and by a Faculty Research Grant

from the University of Missouri-Kansas City. We are grateful to the critical reading of the manuscript by Dr. Paul Rulis.

References and Notes

(1) Eisenberg, A.; Yeager, H. L. In *Perfluorinated Ionomer Membranes*; ACS Symposium Series 180; American Chemical Society: Washington, DC, 1982.

(2) For reviews of proton exchange membranes in fuel cell applications, see: Crabtree, G. W.; Dresselhaus, M. S.; Buchanan, M. V. *Phys. Today* **2004**, *57*, 39. Eikerling, M.; Kornyshev, A. A.; Kucernak, A. R. *Phys. Today* **2006**, *59*, 38.

(3) Heitner-Wirguim, C. *J. Membr. Sci.* **1996**, *120*, 1.

(4) Will, F. G. *J. Electrochem. Soc.* **1979**, *126*, 36.

(5) Will, F. G.; Spacil, H. S. *J. Power Sources* **1980**, *5*, 173.

(6) Yeager, H. L.; Kipling, B.; Dotson, R. L. *J. Electrochem. Soc.* **1980**, *127*, 303.

(7) Jorne, J. *J. Electrochem. Soc.* **1982**, *129*, 722.

(8) Loppinet, B.; Gebel, G.; Williams, C. E. *J. Phys. Chem. B* **1987**, *101*, 1884.

(9) Gebel, G.; Moore, R. B. *Macromolecules* **2000**, *33*, 4850.

(10) Elliott, J. A.; Hanna, S.; Elliott, A. M. S.; Cooley, G. E. *Macromolecules* **2000**, *33*, 4161.

(11) James, P. J.; Elliott, J. A.; McMaster, T. J.; Newton, J. M.; Elliott, A. M. S.; Hanna, S.; Miles, M. J. *J. Mater. Sci.* **2000**, *35*, 5111.

(12) James, P. J.; McMaster, T. J.; Newton, J. M.; Miles, M. J. *Polymer* **2000**, *41*, 4223.

(13) Sodaye, H. S.; Pujari, P. K.; Goswami, A.; Manohar, S. B. *J. Polym. Sci., B* **1997**, *35*, 771; *ibid* **1998**, *36*, 983.

(14) Dlubek, G.; Buchhold, R.; Hubner, C.; Nakladal, A. *Macromolecules* **1999**, *32*, 2348.

(15) Laurer, J. H.; Winey, K. I. *Macromolecules* **1999**, *32*, 6221.

(16) Chomakova-Haefke, M.; Nyffenegger, R.; Schmidt, E. *Appl. Phys. A* **1994**, *59*, 151.

(17) McLean, R. S.; Doyle, M.; Sauer, B. B. *Macromolecules* **2000**, *33*, 6541.

(18) Lehmani, A.; Durand-vidal, S.; Turq, P. *J. Appl. Polym. Sci.* **1998**, *68*, 503.

(19) Nguyen, T. V.; Nguyen, M. V.; Lin, G.; Rao, N.; Xie, X.; Zhu, D-M. *Electrochem. Solid-State Lett.* **2006**, *9*, A88−91.

(20) Hsu, W. Y.; Gierke, T. D. *J. Membr. Sci.* **1983**, *13*, 307.

(21) Gierke, T. D.; Gunn, G. E.; Wilson, F. C. *J. Polym. Sci. Polym Phys.* **1981**, *19*, 1687.

(22) Eisenberg, A.; Hird, B.; Moore, R. B. *Macromolecules* **1990**, *23*, 4098.

(23) Anantaraman, A. V.; Gardner, C. L. *Electroanal. J. Chem* **1996**, *414*, 115.

(24) Choi, P.; Jalani, N. H.; Datta, R. *J. Electrochem. Soc.* **2005**, *152*, E84.

(25) Rollet, A. L.; Diat, O.; Gebel, G. *J. Phys. Chem. B* **2002**, *106*, 3033.

(26) Gebel, G. *Polymer* **2000**, *41*, 5829.

(27) Porat, R.; Fryer, J. R.; Huxham, M.; Rubinstein, I. *J. Phys. Chem.* **1995**, *99*, 4667.

(28) Bussian, David A.; O'Dea, James R.; Metiu, Horia; Buratto, Steven K. *Nano Lett.* **2007**, *7*, 227.

(29) Isolevich, A. S.; Kornyshev, A. A.; Steinke, J. H. G. *J. Phys. Chem. B* **2004**, *108*, 11953.

(30) Yang, Y.; Holdcroft, S. *Fuel Cells* **2005**, *5*, 171.

(31) Fan, F.-R. F.; Bard, A. J. *Science* **1995**, *270*, 1849.

(32) Bath, B. D.; Lee, R. D.; White, H. S. *Ana. Chem.* **1998**, *70*, 1047.

(33) O'Hayre, R.; Lee, M.; Prinz, F. B. *J. Appl. Phys.* **2004**, *95*, 8382.

(34) *NanoScan System*; Molecular Imaging Corp.: Tempe, AZ.

(35) Yang, C.; Srinivasan, S.; Bocarsly, A. B.; Tulyani, S.; Benziger, J. B. *J. Membr. Sci.* **2004**, *237*, 145.

(36) Priour, D. Private communications.

(37) Guckenberger, R.; Heim, M.; Cevc, G.; Knapp, H.; Wiegraebe, W.; Hillebrand, A. *Science* **1994**, *266* 1538.